



# PDPN/CCL2/STAT3 feedback loop alter CAF heterogeneity to promote angiogenesis in colorectal cancer

Die Yu<sup>2,3</sup> · Hanzheng Xu<sup>2,3</sup> · Jinzhe Zhou<sup>1</sup> · Kai Fang<sup>2,3</sup> · Zekun Zhao<sup>1</sup> · Ke Xu<sup>4,5</sup>

Received: 1 May 2024 / Accepted: 31 July 2024  
© The Author(s), under exclusive licence to Springer Nature B.V. 2024

## Abstract

Colorectal cancer (CRC) is one of the common clinical malignancies and the fourth leading cause of cancer-related death in the world. The tumor microenvironment (TME) plays a crucial role in promoting tumor angiogenesis, and cancer-associated fibroblasts (CAFs) are one of the key components of the tumor microenvironment. However, due to the high heterogeneity of CAFs, elucidating the molecular mechanism of CAF-mediated tumor angiogenesis remained elusive. In our study, we found that there is pro-angiogenic functional heterogeneity of CAFs in colorectal cancer and we clarified that Podoplanin (PDPN) can specifically label CAF subpopulations with pro-angiogenic functions. We also revealed that PDPN+CAF could maintain CAF heterogeneity by forming a PDPN/CCL2/STAT3 feedback loop through autocrine CCL2, while activate STAT3 signaling pathway in endothelial cells to promote angiogenesis through paracrine CCL2. We demonstrated WP1066 could inhibit colorectal cancer angiogenesis by blocking both the PDPN/CCL2/STAT3 feedback loop in CAFs and the STAT3 signaling pathway in endothelial cells. Altogether, our study suggests that STAT3 could be a potential therapeutic target for blocking angiogenesis in colorectal cancer. We provide theoretical basis and new therapeutic strategies for the clinical treatment of colorectal cancer.

**Keywords** CAF · CRC · Angiogenesis · PDPN · STAT3

Die Yu, Hanzheng Xu and Jinzhe Zhou contributed equally to this work.

- ✉ Kai Fang  
fangkai94ok@163.com
- ✉ Zekun Zhao  
doctor999zack@163.com
- ✉ Ke Xu  
kexu@shu.edu.cn; cola519@163.com

- <sup>1</sup> Department of General Surgery, Tongji Hospital, School of Medicine, Tongji University, Shanghai 200065, China
- <sup>2</sup> State Key Laboratory of Bioreactor Engineering, Shanghai Key Laboratory of New Drug Design, School of Pharmacy, East China University of Science and Technology, 130 Meilong Rd, Shanghai 200237, China
- <sup>3</sup> Department of General Surgery, Putuo Hospital, Shanghai University of Traditional Chinese Medicine, Shanghai 200062, China
- <sup>4</sup> Institute of Translational Medicine, Shanghai University, Shanghai 200444, China
- <sup>5</sup> Wenzhou Institute of Shanghai University, Wenzhou, China

## Introduction

Colorectal cancer (CRC) is one of the clinically common malignant tumors originating from the mucosal epithelium of the colorectum [1]. CRC is the third most common malignant tumor and the fourth leading cause of cancer deaths in the world, with nearly 2 million new cases and 1 million deaths worldwide each year [2, 3]. It is now widely accepted that the tumor stroma plays a key role in tumorigenesis, progression, drug resistance. In colorectal cancer, the tumor stroma consists of a variety of cell types (immune cells, endothelial cells, cancer-associated fibroblasts etc.), among which cancer-associated fibroblasts (CAFs) are the most abundant. CAFs are not only the major mesenchymal cells in the tumor microenvironment [4], but also important regulators of cancer development and progression. CAFs are capable of secreting cytokines, growth factors, and other activators to shape the tumor microenvironment. They stimulate tumor growth, alter inflammatory responses, remodel ECM environment and promote metastasis, thus affecting the clinical prognosis of colorectal cancer [5, 6].

Different cell origins and different marker expression make CAFs behave as a highly heterogeneous cell subset. Single-cell RNA sequencing technology (scRNA-seq) has revealed that the main feature of the CAF phenotype is the increased expression of markers such as  $\alpha$ -smooth muscle actin ( $\alpha$ -SMA), fibroblast activation protein (FAP), fibroblast specific protein 1 (FSP1), and Vimentin (VIM) [7]. However, one of the main reasons hindering progress in the field of CAF research is the lack of precision in the identification of CAF-specific markers [8]. In addition, CAF also exhibits biological heterogeneity in terms of function [9, 10], which leads to different CAF subpopulations exhibiting different or even opposite functional roles in the tumor microenvironment. Therefore, we urgently need a comprehensive understanding of the heterogeneity of CAFs in CRC, and then gain a deeper understanding of the specific mechanisms of CAFs in the progression of colorectal cancer.

In this study, we thoroughly investigated the heterogeneity of pro-angiogenic function of CAF from different colorectal cancer patients and the mechanisms leading to this functional heterogeneity. We clarified that PDPN can serve as a specific marker of CAF subsets with strong pro-angiogenic function, and that increased expression of PDPN in CAFs is positively correlated with angiogenic function. In addition, we elucidated the mechanism by which CAF with high PDPN expression exerts promoting angiogenic effects, and systematically demonstrated that PDPN-CCL2-STAT3 feedback loop in CAF not only promotes angiogenesis through paracrine CCL2, but also maintains CAFs heterogeneity through autocrine CCL2. More importantly, we found that STAT3 inhibitor WP1066 could effectively inhibit the pro-angiogenic effect mediated by CAF heterogeneity and may be a new therapeutic target for colorectal cancer to inhibit tumor metastasis.

## Materials and methods

### Isolation, culture and identification of CAFs

The specimens were collected from tumor tissue specimens of CRC patients (4 patients) excised during surgery in Putuo Affiliated Hospital. The pathological diagnosis was moderately differentiated adenocarcinoma of the colon. All specimens were fresh and complete, including epithelial tissue and their adjacent connective tissue, which were clinically and pathologically confirmed. We placed the specimen in a petri dish, excess fat and residual tissues were removed from the edge, the tissues were washed with PBS containing 1% penicillin/streptomycin, chopped and transferred to a 15 ml centrifuge tube, centrifuged for 5 min, the

supernatant was discarded, added collagenase 5 times the volume of the tissue block. Then, the tissue was digested in shaker at 37 °C for 1 h. After centrifugation for 5 min under the above conditions, collagenase was discarded, 2 ml of complete medium containing 15% FBS was added, and discrete pieces of tissue were removed and centrifuged for 5 min (this step was repeated 3 times). After removing all collagenase, the medium was added and transferred to small petri dishes, which were then incubated in an incubator. When the fibroblasts grow in a divergent manner around the tissue block, normal digestion and passage could be performed. Biological identification was carried out by morphological observation and detection of CAF markers by WB experiments.

### Cell Culture

The human cell lines applied in the experiment were HCT116 and HUVECs. HCT116 cells (ATCC, Manassas, VA) were cultured in RPMI1640 medium containing 10% FBS alongside 1% penicillin/streptomycin. Human umbilical vein endothelial cells (HUVECs; #8000, ScienCell, USA) were grown in endothelial cell medium (ECM; #1001, ScienCell, USA). Cells were cultured in a humidified incubator with standard culture conditions of 5% CO<sub>2</sub> at 37 °C under normal oxygen conditions.

### BrdU

We collected medium of the cells treated with different CAFs' conditioned medium to determine the cell proliferation of HUVECs. Then the samples were subjected to ELISAs using BrdU Cell Proliferation ELISA Kit (Abcam) to determine the cell proliferation of HUVECs, according to manufacturer's procedures.

### Tube formation

HUVECs were incubated with conditioned medium for 24 h and then treated with the tube formation assay. Matrigel (BD, #356234, USA) was thawed overnight at 4 °C, and 50  $\mu$ l of Matrigel was spread in a 96-well plate and polymerized for 30 min at 37 °C. Next,  $3 \times 10^4$  HUVECs in 50  $\mu$ l of ECM were spread into each well for incubation for 4 h at 37 °C in 5% CO<sub>2</sub>. HUVECs were observed and photographed under a microscope.

### Cell migration assay

HUVECs were incubated with conditioned medium for 24 h before the migration assay. HUVECs suspension ( $1 \times 10^5$ ) in 300  $\mu$ l of serum-free ECM were mixed into the chamber

(8.0 µm pore size, #353,097, FALCON, USA), and allowed to migrate towards 700 µl of complete ECM. The unigrated cells were removed from the upper part of the Transwell chamber with a cotton swab after 6 h of incubation, and the insert was fixed with 3.7% paraformaldehyde for 15 min at room temperature. The Transwell inserts were stained with 500 µl of 1x crystal violet solution for 30 min at 37 °C. Then, the insert was immersed in PBS and washed three times with PBS for 5 min each time, and then dried and photographed under a microscope.

### Adhesion assay

HUVECs were spread in a 24-well plate and then treated with conditioned medium for 24 h. HCT116/GFP cells ( $1 \times 10^6$ ) in 300 µl of serum-free ECM were coincubated with the treated HUVECs for incubation at 37 °C for 2 h. Cells were washed with PBS three times and then photographed under a fluorescence microscope.

### Western blot

The cells were first lysed using RIPA lysis buffer and then centrifuged at 12,000 rpm for 15 min at 4 °C. Bicinchoninic acid (BCA) assays (Beyotime) were used to quantitate the proteins. The proteins were subjected to SDS-PAGE, followed by being blocked with nonfat milk for 1 h at room temperature. Then incubated with specific primary antibodies (Actin, ab6276, Abcam), (FAP, 3195s, CST), (Vimentin, ab92547, Abcam), (VEGFA, ab92536, Abcam), (ICAM, ab2213, Abcam), (SELE, BBA16, R&D), (SELP, ab255822, Abcam), (STAT3, 9139s, CST), (P-STAT3, ab76315, Abcam), (AKT, ab179463, Abcam), (P-AKT, 4060 S, CST), (PDPN, ab10288, Abcam), (β-catenin, 610154, BD), (Lamin B, 6581-1, Epitomics) 4 °C overnight. After being washed for three times with 1×TBST, the membranes were incubated with horseradish peroxidase (HRP)-conjugated secondary antibodies (Abcam ab6721/ab6789) at room temperature for 1 h. The protein bands were detected using ChemiDOc MP Chemiluminescence Gel Imaging system (Bio-Rad) and then obtained by ImageJ software.

### Immunofluorescence

The cultured cells were fixed in 4% paraformaldehyde/PBS for 10 min, removed and placed in 0.2% Triton X-100 for half an hour, and then sealed with 100% FBS for 60 min. The fixed cells were then incubated with a primary antibody specific for FAP, CD31, ERG, DAPI, β-catenin, p-STAT3, Merge (Cell Signaling Technology, Inc.), followed by a

secondary antibody. Images were captured by using a confocal laser-scanning microscope (LSM 510; Carl Zeiss, Inc).

### Immunohistochemistry

The collected tissue samples were fixed with 10% formalin, embedded in paraffin, and sliced (5-mm thick). Immunohistochemistry of FAP, CD31, ERG, PDPN, β-catenin, p-STAT3 was conducted. The slides were dewaxed and incubated with 3% H<sub>2</sub>O<sub>2</sub> solution for 10 min. The antigens were detected by the heat-induced antigen retrieval method. Tissues were incubated with 5% BSA at 37 °C for half an hour and then incubated with primary antibodies in PBS at 4 °C overnight. The secondary antibodies were applied for 30 min at 37 °C by the indirect avidin-biotin-peroxidase method. The bound antibodies were developed by the EnVision (K4007, Dako) signal enhancement system. Sections were counterstained with Harris haematoxylin, dehydrated and mounted. The expression in cells with positive staining was quantified from 10 random images per experimental group under a microscope (Leica).

### Immunoscore method

The immunohistochemical staining results were assigned a mean score considering both the intensity of staining and the proportion of tumor cells with an unequivocal positive reaction. Each section was independently assessed by 2 pathologists without prior knowledge of patient data. Positive reactions were defined as those showing brown signals in the cell cytoplasm. A staining index (values, 0–12) was determined by multiplying the score for staining intensity with the score for positive area. The intensity was scored as follows: 0, negative; 1, weak; 2, moderate; and 3, strong. The frequency of positive cells was defined as follows: 0, less than 5%; 1, 5–25%; 2, 26–50%; 3, 51–75%; and 4, greater than 75%.

### ELISA

CCL2 in CAF culture supernatants was evaluated by a Human CCL2 ELISA Kit (Solarbio, Beijing) according to the manufacturer's protocol. CCL2 in serum was evaluated by a Mouse CCL2 ELISA Kit (Boster, USA) according to the manufacturer's protocol.

### RT-qPCR

Total RNA was extracted with TRIzol (Invitrogen), and the concentration was quantitated by measuring the absorbance at 260 nm. Reverse transcription was conducted using the PrimeScript RT-PCR Kit (TaKaRa Biotechnology)

according to the instructions of the manufacturer. Quantitative RT-PCR was carried out by using the PrimeScript RT-PCR Kit according to the procedures of specification. The PCR primers' sequences were as follows:

CCL2, 5'-CAGCCAGATGCAATCAATGCC-3' and 5'-TGGAATCCTGAACCCACTTCT-3'.

PDPN, 5'-AACCAGCGAAGACCGCTATAA-3' and 5'-CGAATGCCTGTTACTACTGTTGA-3'.

VEGFA, 5'-ACTGTCAGACCACGGAATGAT-3' and 5'-GGGCAAGATTTTACGCCACATAC-3'.

ICAM-1, 5'-ATGCCAGACATCTGTGTCC-3' and 5'-GGGGTCTCTATGCCCAACAA-3'.

PDGFA, 5'-TGGCAGTACCCCATGTCTGAA-3' and 5'-CCAAGACCGTCACAAAAGGC-3'.

SELE, 5'-ATGTTCAAGCCTGGCAGTTCCG-3' and 5'-GCAGAGCCATTGAGCGTCCATC-3'.

SELP, 5'-CGCTCTGGACCAACCCTGTTTC-3' and 5'-CTCCTGGCTTCTGTGGCTTGTG-3'.

### Clustering and marker gene identification

Based on the single-cell reference expression quantification public dataset, the correlation of the cell expression profile to be identified with the reference dataset was calculated by SingleR package. In order to eliminate artificial subjective factors as much as possible, the cell type with the highest correlation in the reference dataset was assigned to the cell to be identified. The identification principle was as follows: Calculate the spearman correlation between the expression profile of each cell annotated in the reference dataset and the expression profile of each cell in the sample, and select the cell type in the dataset with the greatest correlation with the expression of the sample cell as the final cell type to be identified. Marker gene identification uses the FindAllMarkers function in the Seurat package, find genes differentially upregulated by each cell classification relative to other cell populations, and these genes are potential Marker genes for each cell classification. The Marker genes identified were visualized using Feature Plot function.

### GSEA enrichment analysis

GO and KEGG enrichment analysis between the two groups was completed through GSEA using the C5 GO gene set and the C2 KEGG gene set from the MSigDB data (<http://www.gsea-msigdb.org/gsea/msigdb>).

### Cytokine chip

Proteome Profiler Human Angiogenesis Array Kit (R&D) was used. Serum-free DMEM was used to collect CAF62 and CAF95 cell conditioned medium, and 500  $\mu$ l of cell

culture supernatant was run on each array separately. The levels of angiogenesis-related proteins in each array were detected according to the kit instructions.

### In vivo optical imaging

Sodium phenobarbital was injected into the abdominal cavity of mice to play an anesthetic role. Inject D-fluorescein solution into the abdominal cavity 5 min before imaging. The exposure time set during imaging is 20 s, which can be adjusted appropriately according to the exposure intensity. The corresponding wavelengths are 490 and 535 nm.

### Spleen injection liver metastasis model

HCT116-luc + CAFs (1:1) cells were injected into the spleen of 24 male athymic nude mice (4–5 weeks old). During the in vivo experiment, WP1066 (20 mg/kg, selleck) was intraperitoneally injected into the subjects five times every week for 14 days. The body weight was measured every 7 days, and the results were accurately recorded. After WP1066 treatment two weeks, the experimental animals were killed, and the liver and spleen were removed and photographed under white light, then with formalin to provide support for subsequent experiments. Relevant experimental contents and programs were approved by the Ethics Committee of Putuo Hospital.

### PCA principal component analysis

using the FindVariableGenes function in the Seurat package to screen for highly variable genes (HVGs, highly variable genes), and the expression profiles of highly variable genes were used for PCA principal component downscaling analysis. This analysis was completed by sequencing the reference transcriptome of four samples.

### Differentially expressed gene (DEG) analysis and volcano plot analysis

The number of counts (BaseMean value to estimate the expression amount) of each sample gene was standardized by DESeq software, the multiplicity of differences was calculated, and the significance of differences in the number of reads was tested by using NB (Negative Binomial Distribution Test), and the differentially expressed protein coding genes were subject to the final screening based on the multiplicity of differences and the results of the significance of differences test. Differentially expressed genes were shown the distribution by drawing volcano plots, with non-significantly different genes in gray and significantly

different genes in red and green; the horizontal axis is  $\log_2$ FoldChange and the vertical axis is  $-\log_{10}$ pValue.

### GO enrichment analysis

All the protein-coding genes were used as the background list, and the list of differentially encoded genes was used as a candidate list filtered out from the background list. pValue, which represented the significant enrichment or not of the GO function sets in the list of differentially encoded genes, were computed by using the hypergeometric distribution test. pValue was further corrected by Benjamini & Hochberg's multiple test.

### KEGG enrichment analysis

KEGG is a major public database related to Pathway, and the KEGG database was utilized to perform the Pathway analysis of the differential protein coding genes (in combination with the results of the KEGG annotations) and the significance of differential gene enrichment in each Pathway entry was calculated by means of the hypergeometric distribution test.

### Statistical analysis

The GraphPad Prism 8 software was applied to conduct statistical analysis on relevant experimental data. The experimental data were described by means of mean  $\pm$  standard deviation. The results of the two groups were tested by unpaired t-test. ANOVA and Tukey tests were used to test the results of multiple groups, and the level of significant difference was set as  $*P < 0.05$ ,  $**P < 0.01$ ,  $***P < 0.001$ .

## Results

### CAFs from colorectal cancer specimens present functional heterogeneity in promoting angiogenesis

Many studies have shown that CAFs are a type of stromal cells with phenotypic heterogeneity and functional diversity [6, 10]. Particularly, in the function of promoting angiogenesis, Bartoschek et al. found vascular CAFs (vCAFs) exhibiting enriched vascular development in the genetically engineered MMTV-PyMT breast cancer mouse model, implying that CAFs have different subpopulations in terms of promoting angiogenesis [11]. However, there are few reports on the specific mechanism of altering the pro-angiogenic functional heterogeneity of CAFs in CRC.

Fibroblast activation protein (FAP) is a common marker of CAFs, and it has been suggested that FAP expression in CAFs may be associated with tumor angiogenesis. To determine whether FAP could be a specific marker of CAFs with pro-angiogenic function, we collected 19 clinical specimens of colorectal cancer (CRC) and characterized the expressions of FAP (CAF marker) and CD31 (endothelial cell marker) in CRC clinical specimens by immunohistochemistry and immunofluorescence. We found that FAP<sup>+</sup> CAFs (FAP-positive CAFs) and FAP<sup>-</sup> CAFs (FAP-negative CAFs) were positively correlated with the expression of CD31, but FAP<sup>low</sup> CAFs (FAP-low-expression CAFs) and FAP<sup>high</sup> CAFs (FAP-high-expression CAFs) had no significant correlation with the expression of CD31 (Fig. 1A-F). This means that FAP cannot specifically label CAF subpopulations with pro-angiogenic function, indicating that there may be other markers.

To further explore the pro-angiogenic functional heterogeneity of CAFs in CRC, we extracted primary CAFs from colorectal cancer tissue specimens from different patients and named them CAF62, CAF804, CAF95 and CAF540 (Fig. S1A, B). To assess the pro-angiogenic effects of different CAFs, a co-culture method including human umbilical vein endothelial cells (HUVECs) and conditioned medium (CM) derived from different CAFs was employed. We found that the angiogenesis, adhesion and migration abilities of HUVEC were significantly enhanced by CM from CAF95 and CAF540 compared to CAF62 and CAF804, but there was no significant difference in promoting vascular proliferation between them (Fig. 1G, H, Fig. S1C-E). Next, in order to further clarify the mechanism of CAF stimulating HUVEC to promote angiogenesis, we examined the expression levels of angiogenesis-related proteins (VEGFA, SELE, SELP, and ICAM-1) and STAT3 signaling pathway in HUVEC stimulated with different CAF-conditioned medium (CM). Western blotting and qPCR results confirmed that CAF95-CM and CAF540-CM could significantly stimulate STAT3 signal activation and promote the expression of angiogenesis-related proteins in HUVEC compared to CAF62-CM and CAF804-CM (Fig. 1I, J, Fig. S1F). Taken together, CAF from different colorectal cancer tissue specimens showed functional heterogeneity in terms of promoting angiogenesis. Therefore, the above data indicate that we can find specific markers of CAF to further reveal the potential mechanism of CAFs functional heterogeneity in terms of promoting angiogenesis.

### High PDPN expression in CAFs is closely associated with tumor angiogenesis

To gain insights into the mechanism of the heterogeneity in CAFs-mediated angiogenic function, transcriptome analysis

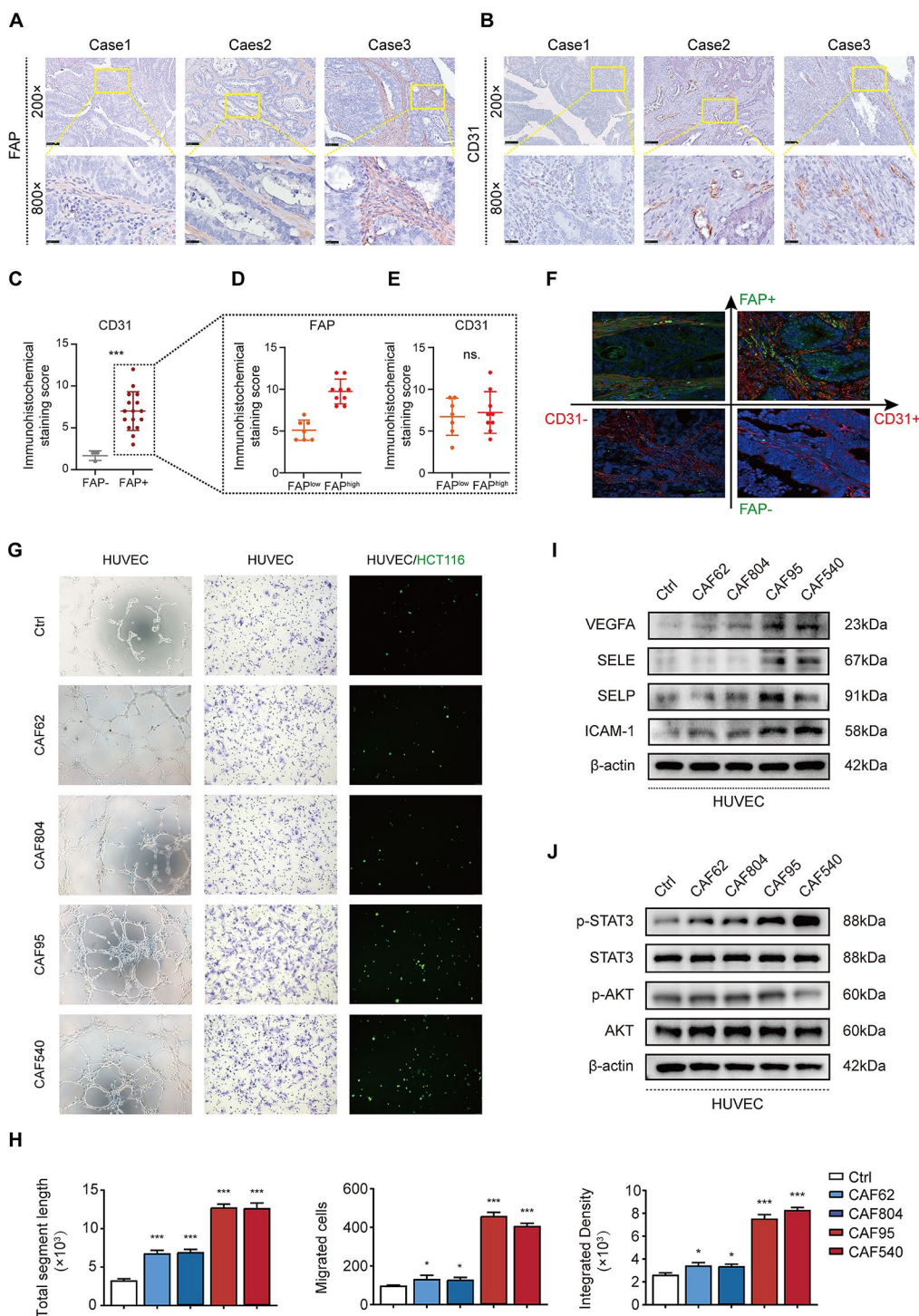


**Fig. 1** CAFs from different colorectal cancer patient specimens present different effect of promoting angiogenesis **(A)** IHC staining score of FAP dividing CRC specimens into FAP negative group (FAP<sup>-</sup>), FAP low expression group (FAP<sup>low</sup>) and FAP high expression group (FAP<sup>high</sup>). Representative FAP images, scale bar: 100  $\mu$ m and 25  $\mu$ m. **(B)** CD31 expression in CRC specimens of FAP<sup>-</sup>, FAP<sup>low</sup> and FAP<sup>high</sup> colorectal cancer specimens by IHC. Representative CD31 images, scale bar: 100  $\mu$ m and 25  $\mu$ m. **(C-E)** Pathological score of IHC staining

for FAP and CD31 in different FAP expression groups. **(F)** IF staining of FAP (green) and CD31 (red) on different patients' tissues. **(G-H)** Tube formation, adhesion, migration of HUVECs treated with CAF-CMs derived from different patients. **(I-J)** WB showing the expression of angiogenesis-related proteins VEGFA, SELE, SELP, and ICAM-1 and angiogenesis-related signaling pathway proteins AKT, p-AKT, STAT3, and p-STAT3 in HUVECs treated with CAF-CMs derived from different patients. The results are presented as the mean (SD)

of CAFs was performed. The four clusters were divided into two subpopulations by principal component analysis (PCA), respectively CAF95, CAF540 and CAF62, CAF804 (Fig. 2A). Volcano plot data showed 601 differentially expressed genes (DEGs) between the two subpopulations (Fig. S2A). Next, Gene Ontology (GO) enrichment analysis and Kyoto Encyclopedia of Genes and Genomes (KEGG) pathway analysis showed that two CAF subpopulations mainly have functional differences in angiogenesis, cytokines, extracellular matrix, Wnt and other signal pathways (Fig. 2B, C). Of note, PDPN (a CAF marker) was highly expressed in CAF subpopulation with pro-angiogenic function (CAF95, CAF540) (Fig. 2D). Moreover, it has been reported that the high PDPN expression of CAF is related to the tumor malignancy and poor prognosis in some cancers [12–16]. Likewise, previous study has shown that the high PDPN expression in human lung squamous cell carcinoma can enhance tumor vascularization [17]. However, there are no studies to clarify whether the high PDPN expression of CAF is a key factor in promoting angiogenesis in colorectal cancer.

In order to determine whether PDPN could serve as a specific marker of CAF with pro-angiogenic function, we found that the expression level of PDPN in CAF95 and CAF540 which have pro-angiogenic function was higher than that in CAF62, CAF804 and NF (Normal Fibroblast) (Fig. 2E, Fig. S2B, C). Therefore, we sorted CAF95 and CAF540 as PDPN<sup>high</sup> CAF, CAF62 and CAF804 as PDPN<sup>low</sup> CAF. Besides, it has been reported that PDPN can enhance Wnt/ $\beta$ -catenin signaling at different levels of the signaling cascade [18]. In the Wnt signal pathway, the entry of its core protein molecule  $\beta$ -catenin into the nucleus is an important prerequisite for activating downstream transcription factors. The activated Wnt/ $\beta$ -catenin signaling pathway can lead to nuclear translocation of  $\beta$ -catenin and promote the expression of angiogenesis-related genes to drive angiogenesis [19]. To this end, we verified that PDPN<sup>high</sup> CAF could increase the nuclear translocation of  $\beta$ -catenin by Western blotting and immunofluorescence (Fig. 2E, F), which suggests that the PDPN/ $\beta$ -catenin signaling axis may be the mechanism of CAFs-mediated promoting angiogenesis. We also further observed STAT3 phosphorylation increased in PDPN<sup>high</sup> CAF (Fig. 2E, F), which shown in many studies about STAT3 signaling pathway promoting angiogenesis and tumor development in CAF [20].

To further verify whether the high PDPN expression is a key factor in the pro-angiogenic function of CAF, we knockdown PDPN in CAF95 (PDPN<sup>high</sup> CAF) to observe its functional changes in CAF with high PDPN expression. We verified that PDPN knockdown in CAF95 could inhibit the transport of  $\beta$ -catenin into the nucleus and STAT3 phosphorylation (Fig. 2G, H). At the same time, we found that PDPN

knockdown inhibited the angiogenesis, adhesion and migration of HUVEC in CAF95 compared to the control group (Fig. 2I–K). The expression of mRNA and protein related to pro-angiogenesis was also down-regulated (Fig. S2D, E). Over all, these data demonstrated that PDPN is a key factor affecting the pro-angiogenic function of CAF. Moreover, our study confirmed that Wnt/ $\beta$ -catenin and STAT3 signal pathway are activated in PDPN<sup>high</sup> CAF, which in turn exert the role of promoting angiogenesis.

### PDPN<sup>high</sup> CAF promotes angiogenesis through the PDPN/CCL2/STAT3 feedback loop

Cytokines and chemokines are the key factors in promoting angiogenesis. Based on the results of GO and KEGG enrichment analysis, we found that there were functional differences in chemokine signaling pathway between PDPN<sup>high</sup> CAF and PDPN<sup>low</sup> CAF. To determine the critical role of chemokines in the pro-angiogenic function of CAF, we evaluated the secretion of pro-angiogenic release factors in CAF62 (PDPN<sup>low</sup> CAF) and CAF95 (PDPN<sup>high</sup> CAF) by cytokine chip, CCL2 showed the most significant differential expression (Fig. 3A), RT-qPCR and ELISA experiments have also further verified (Fig. 3B, Fig. S4A). Furthermore, we found that neutralizing CCL2 expression significantly reduced the pro-angiogenic effect of PDPN<sup>high</sup> CAF and the expression of pro-angiogenesis related mRNAs and proteins (Fig. 3D–G, Fig. S3A–F). These data demonstrated that CCL2 is indeed a key factor secreted by PDPN<sup>high</sup> CAF to promote angiogenesis. Previous studies have shown that the Wnt/ $\beta$ -catenin signaling pathway can regulate the secretion level of CCL2 [19]. Combined with our above studies, we hypothesized that PDPN<sup>high</sup> CAF promotes angiogenesis by secreting CCL2 through the Wnt/ $\beta$ -catenin signaling pathway. Of note, the expression and secretion of CCL2 can also be regulated by the change of PDPN expression in PDPN<sup>high</sup> CAF (CAF95) (Fig. 3C, Fig. S4B).

In previous reports, chemokine is closely related to STAT3 signaling pathway, and CCL2-CCR2 signaling transduction can induce STAT3 phosphorylation [21, 22]. Therefore, we speculated that PDPN<sup>high</sup> CAF may activate the STAT3 signaling pathway to promote angiogenesis by secreting CCL2. Our results confirmed that neutralizing CCL2 suppress STAT3 phosphorylation in HUVECs (Fig. 3G). In addition, it is worth noting that neutralizing CCL2 could inhibit STAT3 phosphorylation in PDPN<sup>high</sup> CAF and also accompanied by the down-regulation of PDPN expression (Fig. 3H, I). Some research has been reported that STAT3 can directly regulate PDPN expression [23, 24], and we also confirmed that STAT3 knockdown could reduce PDPN expression in CAF (Fig. 3J, K). Besides, STAT3 overexpression greatly returned the expression of PDPN

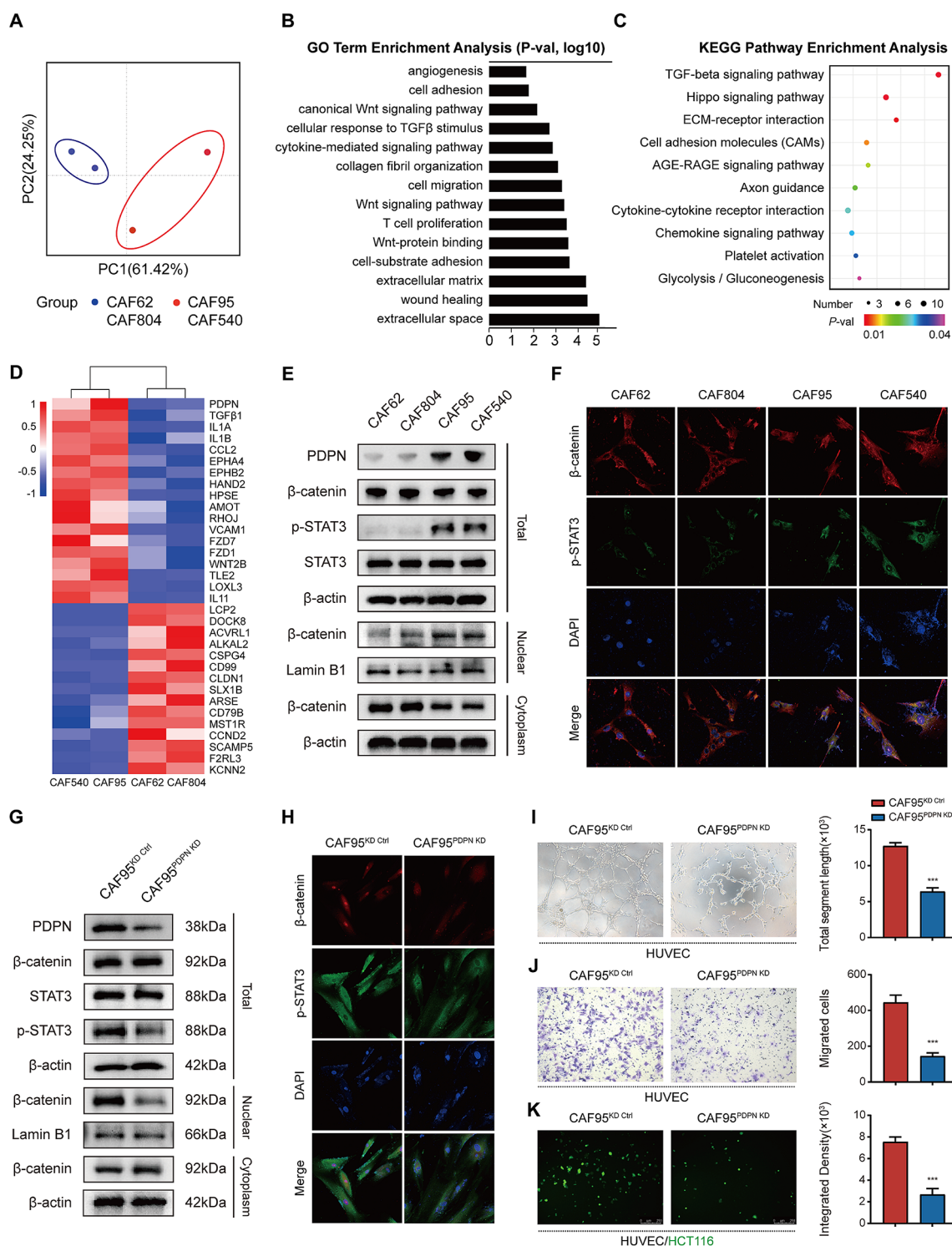


**Fig. 2** High PDPN expression in CAFs is closely associated with tumor angiogenesis. **(A)** PCA principal component analysis of CAFs from different patients by comparing the gene expression profiles of differentially expressed genes (DEGs). PC1 and PC2 are principal components 1 and 2 respectively. **(B-C)** GO enrichment analysis. **(B)** and KEGG pathway enrichment analysis. **(C)** of DEGs between CAF95, CAF540 groups and CAF62, CAF804 groups. **(D)** Heatmap of the DEGs related to functional enrichment between CAF95, CAF540 groups and CAF62, CAF804 groups. **(E)** WB showing the

expression of PDPN,  $\beta$ -catenin, STAT3, and p-STAT3 in total protein, the expression of  $\beta$ -catenin in nuclear and cytoplasm protein between different CAFs. **(F)** IF staining of  $\beta$ -catenin and p-STAT3 in different CAFs. **(G)** WB showing the expression of certain protein in CAF95 after treatment of PDPN knockdown **(H)** IF staining of  $\beta$ -catenin and p-STAT3 in CAF95 after treatment of PDPN knockdown **(I-K)** Tube formation, adhesion and migration of HUVECs treated with CMs derived from CAF95<sup>KD Ctrl</sup> and CAF95<sup>PDPN KD</sup>. The results are presented as the mean (SD)



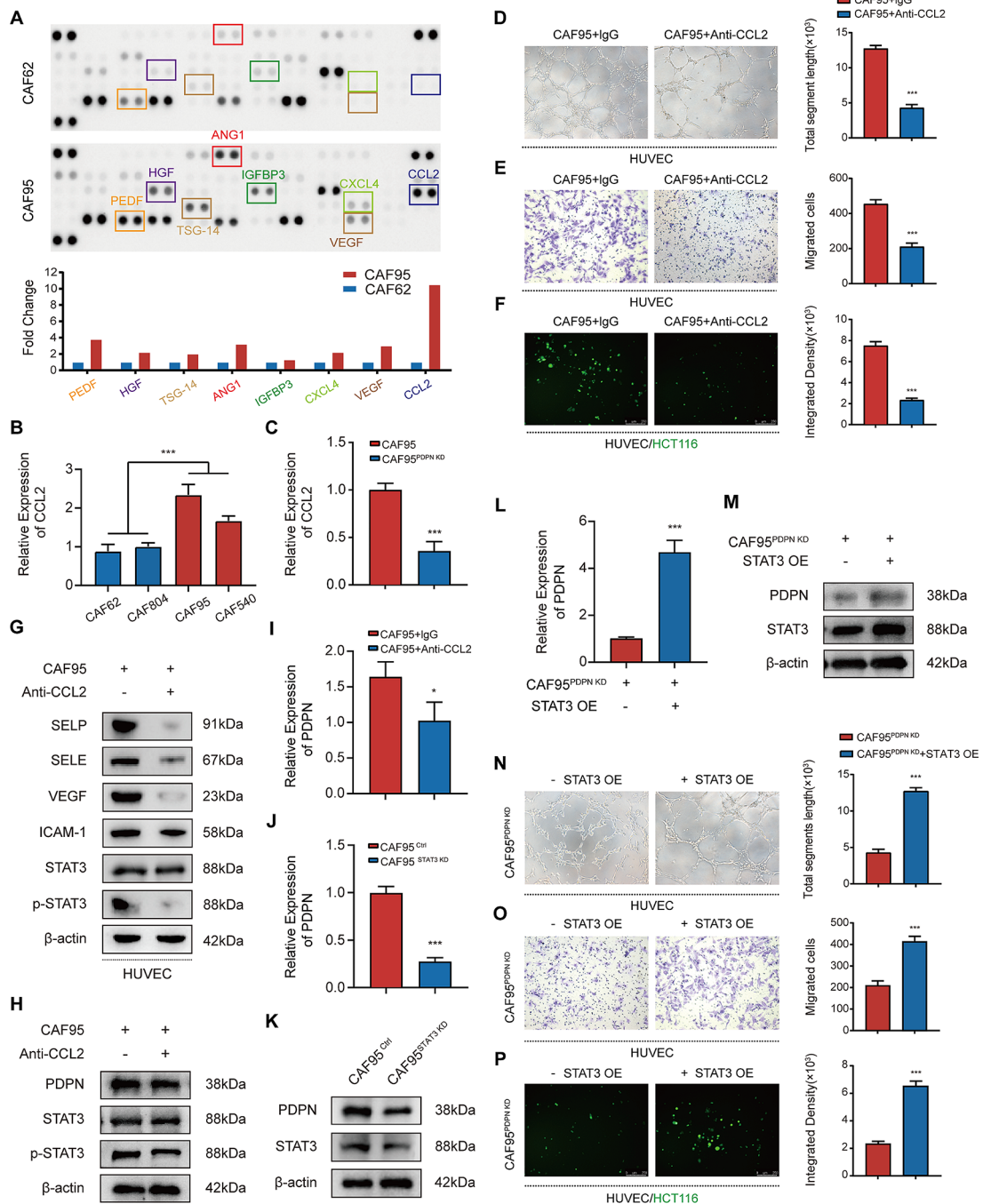


**Fig. 3** PDPN<sup>high</sup> CAF exert pro-angiogenic function through the PDPN/CCL2/STAT3 feedback loop (A) Cytokine Chip detecting relative levels of angiogenesis-related proteins in CAF62 and CAF95. (B) RT-qPCR showing the difference of CCL2 expression from different CAFs. (C) RT-qPCR showing the difference of CCL2 expression between CAF95 and CAF95<sup>PDPN KD</sup>. (D-F) Tube formation, adhesion and migration of HUVECs treated with CMs derived from CAF95 and CAF95 + Anti-CCL2. (G) WB showing the expression of angiogenesis-related proteins VEGFA, SELE, SELP and ICAM-1 and angiogenesis-related signaling pathway proteins STAT3 and p-STAT3 in HUVECs treated with CMs derived from CAF95 + Anti-CCL2. (H) WB showing the protein expression of PDPN, STAT3 and P-STAT3

in CAF95 and CAF95 + Anti-CCL2. (I) RT-qPCR showing the difference of PDPN expression between CAF95 and CAF95 + Anti-CCL2. (J) RT-qPCR showing the difference of PDPN expression between CAF95 and CAF95<sup>STAT3 KD</sup> (K) WB showing the protein expression of PDPN and STAT3 in CAF95 and CAF95<sup>STAT3 KD</sup>. (L) RT-qPCR showing the difference of PDPN expression between CAF95<sup>PDPN KD</sup> and CAF95<sup>PDPN KD</sup> + STAT3 OE. (M) WB showing the protein expression of PDPN and STAT3 in CAF95<sup>PDPN KD</sup> treated with STAT3 over-expression (N-P) Tube formation, adhesion and migration of HUVECs treated with CMs derived from CAF95<sup>PDPN KD</sup> and CAF95<sup>PDPN KD</sup> + STAT3 OE. The results are presented as the mean (SD).

and CCL2 in CAF95 with PDPN knockdown (Fig. 3L, M, Fig. S4D), accompanied by enhanced pro-angiogenic effect of such CAF subgroup (Fig. 3N-P). The secretion level of CCL2 was also returned under the condition of STAT3 overexpression (Fig. S4C). At the same time, we also verified the consistent results in CAF62 (PDPN<sup>low</sup> CAF) by STAT3 overexpression (Fig. S4E-P).

Taken together, these results indicate that PDPN<sup>high</sup> CAF activate the STAT3 signaling pathway to promote angiogenesis through paracrine CCL2 in colorectal cancer. At the same time, PDPN<sup>high</sup> CAF regulate its heterogeneity through autocrine CCL2 to form a PDPN/CCL2/STAT3 feedback loop, thus maintaining the pro-angiogenic functional subtype of CAF.

### PDPN/CCL2/STAT3 feedback loop of CAF promote angiogenesis in human CRC specimens

To further explore the clinical significance of PDPN affecting CAF heterogeneity, unsupervised clustering analysis was performed on 4 clinical tissues specimens of colorectal cancer by single-cell sequencing technique. As shown in Figs. 4A and 9 cell clusters were identified, including Epithelial cells, Endothelial cells (ECs), T cells, CAFs, Dendritic cells (DCs), B cells, Basophils, Neutrophils, and Macrophages (Fig. 4A). The CAFs obtained from the above identification were further analyzed by dimensional reduction and identified into two subpopulations with different expression of PDPN (PDPN<sup>high</sup> CAF and PDPN<sup>low</sup> CAF) (Fig. 4A, B).

Next, we conducted a differential gene expression analysis and GO enrichment analysis to explore how expression states differed between PDPN<sup>high</sup> CAF and PDPN<sup>low</sup> CAF. It was found that the PDPN<sup>high</sup> CAF group showed enrichment of angiogenesis, cell adhesion, and cell migration, as well as significant enrichment of Wnt signaling pathway, chemokine-mediated signaling pathway and JAK-STAT3 signaling pathway. Moreover, PDPN<sup>high</sup> CAF group exhibited increased expression levels of pro-angiogenesis (ANGPTL2, NRP2, COL8A1), Wnt signaling pathway (WNT5A, SFRP2) and JAK-STAT3 signaling pathway (IL11) signature genes (Fig. 4B-E). The above results further confirmed that PDPN<sup>high</sup> CAF was a subpopulation with stronger pro-angiogenic function in human colorectal cancer tissues, and its function was associated with Wnt signaling pathway, chemokine-mediated signaling pathway and JAK-STAT3 signaling pathway.

To test whether PDPN could serve as a specific marker of the pro-angiogenic CAF subpopulation, we analyzed tissue sections from clinical CRC patients ( $n=19$ ). By immunohistochemical analysis, we divided the patient tissues into high PDPN expression group and low PDPN expression

group (PDPN<sup>high</sup> CAF group and PDPN<sup>low</sup> CAF group). The results showed that the expression of p-STAT3 and CD31 in PDPN<sup>high</sup> CAF group were significantly upregulated compared with PDPN<sup>low</sup> CAF group (Fig. 4F, G). Immunofluorescence analysis also revealed that FAP showing co-expression with PDPN, p-STAT3, and CD31 respectively in PDPN<sup>high</sup> CAF group (Fig. S5A). The secretion of CCL2 in the serum of patients was analyzed by ELISA, and the results showed that the serum of patients with high PDPN expression exhibited higher concentration of CCL2 secretion (Fig. 4H). In addition, using The Cancer Genome Atlas-Colon Adenocarcinoma (TCGA-COAD) database, there was a positive correlation between CCL2, CD31 (PECAM) and PDPN expression (Fig. 4I-K). In conclusion, our study demonstrated that PDPN can serve as a marker to identify pro-angiogenic functional heterogeneity of CAF in clinical CRC patient tissues. Moreover, the pro-angiogenesis effect of PDPN/CCL2/STAT3 feedback loop in CAF was also confirmed by clinical CRC tissue specimens.

### Inhibiting STAT3 signaling pathway alter CAF heterogeneity and reduce CRC angiogenesis through PDPN/CCL2/STAT3 Feedback Loop in vitro

Several studies have shown that STAT3 plays a critical role in vascular activation. Recently, it has also been shown that STAT3 is a key factor in the regulation of CAF function and heterogeneity [20, 25]. Our previous results demonstrated that CAF can activate the STAT3 signaling pathway in HUVEC to promote angiogenesis and the existence of PDPN/CCL2/STAT3 feedback loop maintains CAF heterogeneity. Given the dual role of STAT3 signaling pathway in HUVEC and CAF, we selected WP1066 as an inhibitor to target STAT3. We used two different approaches with WP1066 for treatment in vitro: CAF95cm + WP and (CAF95 + WP) cm (As shown in the schematic diagram, cm represents conditional medium). The results showed that both two approaches were able to inhibit the angiogenesis, migration and adhesion of HUVEC (Fig. 5A, B). Meanwhile, the expression of SELE, SELP, ICAM-1, VEGFA and P-STAT3 were decreased significantly by WP1066 treatment (Fig. 5C, D). Of note, we also found that the CAF95cm + WP treatment was more effective than the (CAF95 + WP)cm treatment. We hypothesized that CAF95cm + WP treatment not only directly inhibited STAT3 phosphorylation in HUVECs, but also inhibited STAT3 phosphorylation in HUVECs induced by paracrine CCL2 in CAF95cm. Taken together, we verified that WP1066 could inhibit CAF-mediated pro-angiogenic effect in multiple dimensions.

We have demonstrated that CCL2 plays a key role as a cytokine in the pro-angiogenic function of PDPN<sup>high</sup> CAF. Next, based on ELISA and PCR experiments, we

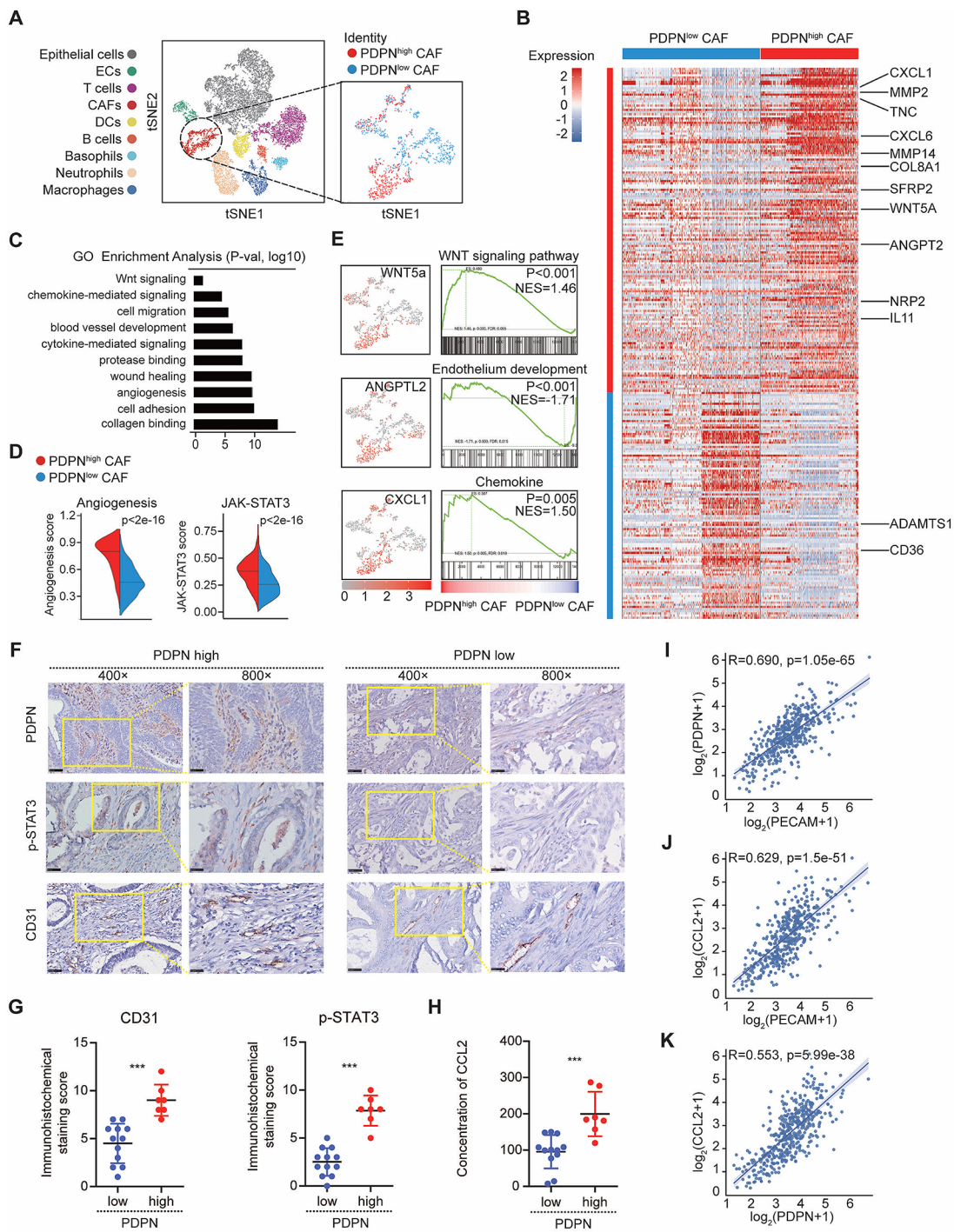


**Fig. 4** PDPN/CCL2/STAT3 feedback loop of CAF promote angiogenesis in human CRC specimens. **(A)** t-SNE dimensionality reduction analysis of human colorectal cancer cells colored by cluster and dot plots showing the expression of PDPN for CAF on the t-SNE map. **(B)** Heatmap analysis of differentially expressed genes in PDPN<sup>high</sup> CAF and PDPN<sup>low</sup> CAF. **(C)** GO functions enrichment analysis of upregulated genes in PDPN<sup>high</sup> CAF versus PDPN<sup>low</sup> CAF. **(D)** Split violin plot of angiogenesis gene signature score and JAK-STAT3 signaling pathway gene signature score in PDPN<sup>high</sup> CAF versus PDPN<sup>low</sup> CAF. **(E)** GSEA analysis of DEGs between PDPN<sup>high</sup> CAF and PDPN<sup>low</sup>

CAF in the terms of “Wnt signaling pathway”, “endothelium development” and “chemokine” **(F)** Representative images of the IHC staining of PDPN, p-STAT3 and CD31 in human CRC tissues, the scale bars are 50 μm and 25 μm. **(G)** Pathological score of IHC staining for CD-31 and P-STAT3 in PDPN<sup>high</sup> and PDPN<sup>low</sup> group of human CRC tissues. **(H)** ELISA detection of CCL2 expression level in serum between PDPN<sup>high</sup> and PDPN<sup>low</sup> group **(I-K)** Correlation analysis among PDPN, CD31 (PECAM) and CCL2 in TCGA-COAD database. The results are presented as the mean (SD).

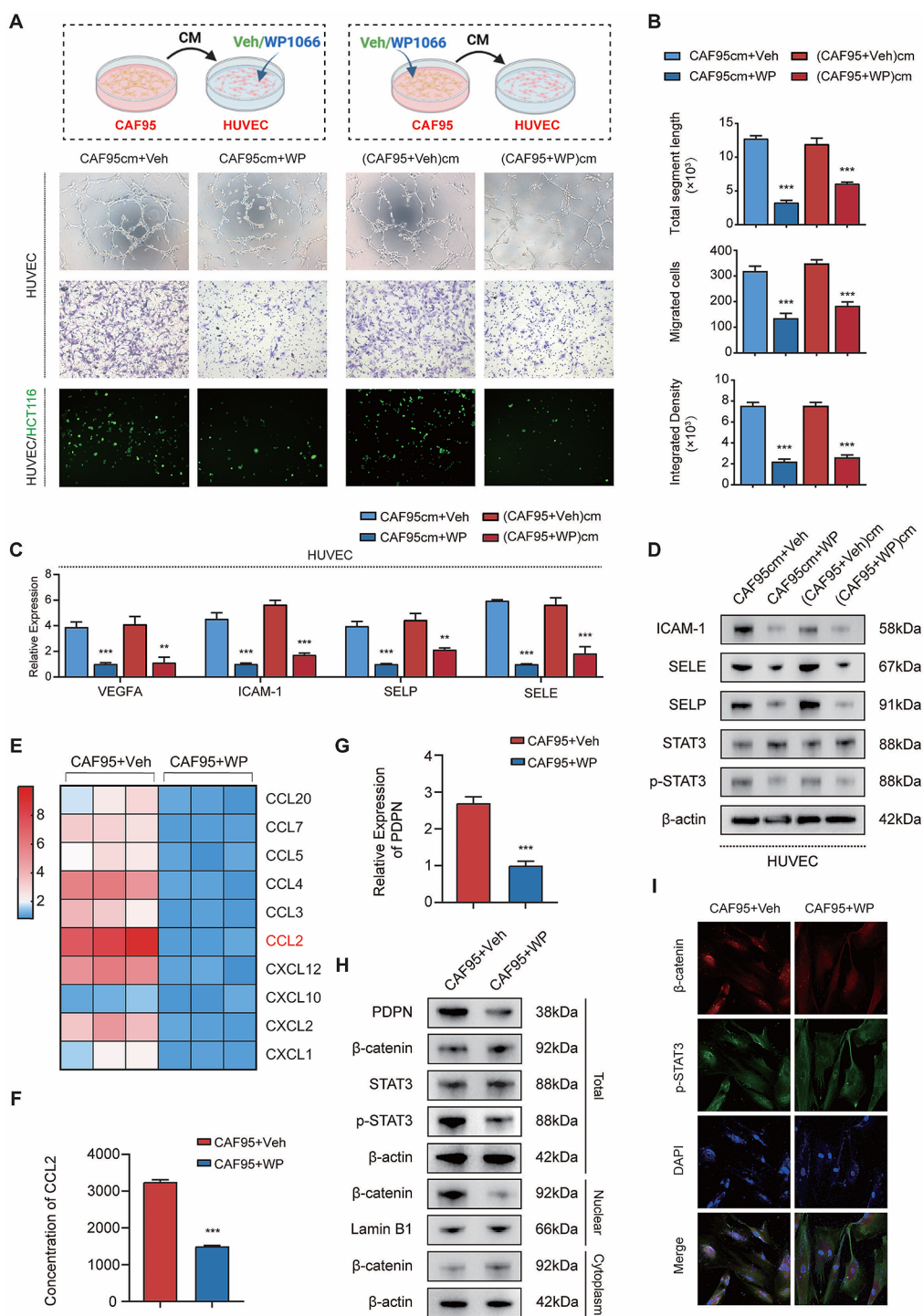


**Fig. 5** WP1066 alters CAF heterogeneity and reduces CRC angiogenesis through PDPN/CCL2/STAT3 Feedback Loop in vitro. **(A–B)** Tube formation, adhesion and migration of HUVECs treated with CAF95cm+Veh/WP1066 and (CAF95+Veh)/WP1066cm. **(C)** qPCR showing the relative expression of VEGFA, ICAM-1, SELE and SELP in HUVECs treated with CAF95cm+Veh/WP1066 and (CAF95+Veh)/WP1066cm. **(D)** WB showing the expression of angiogenic and signaling pathways related proteins in HUVECs treated with CAF95cm+Veh/WP1066 and (CAF95+Veh)/WP1066cm. **(E)** PCR

Heatmap of differentially expressed cytokines in CAF95 treated with Veh/WP1066. **(F)** ELISA detection of CCL2 secretion level in CAF95 treated with Veh/WP1066. **(G)** RT-qPCR showing the expression level of PDPN in CAF95 treated with Veh/WP1066. **(H)** WB showing the expression of PDPN, β-catenin, STAT3, and p-STAT3 in total protein, the expression of β-catenin in nuclear and cytoplasm protein in CAF95 treated with Veh/WP1066. **(I)** IF staining of β-catenin and p-STAT3 in CAF95 treated with Veh/WP1066. The results are presented as the mean (SD)

found that WP1066 could significantly inhibit the secretion and expression of CCL2 in CAF95 (Fig. 5E, F). Notably, PDPN expression and STAT3 phosphorylation in CAF95 were down-regulated after WP1066 treatment, which further revealed that the regulatory effect of STAT3 pathway on PDPN expression in the PDPN/CCL2/STAT3 feedback loop (Fig. 5G-I). The inhibition of  $\beta$ -catenin nuclear translocation also indicated that the down-regulation of PDPN in PDPN<sup>high</sup> CAF exerts an inhibitory effect on the Wnt/ $\beta$ -catenin signaling pathway, thus reducing the secretion of cytokine CCL2. Based on the above results, our study confirmed that WP1066 specifically inhibited STAT3 phosphorylation of CAF *in vitro*, and regulate the Wnt/ $\beta$ -catenin signaling pathway by inhibiting PDPN expression, thus inhibiting the paracrine and autocrine of CCL2. Finally, the heterogeneity of CAF mediated by PDPN/CCL2/STAT3 feedback loop was blocked, and the activation of STAT3 pathway in HUVEC was inhibited, resulting in the inhibition of angiogenesis.

### Inhibiting PDPN/CCL2/STAT3 feedback loop of CAF suppresses tumor metastasis by reducing angiogenesis *in vivo*

Next, to determine the efficacy of the STAT3 inhibitor WP1066 *in vivo*, a liver metastasis model was established by using HCT116 cells expressing luciferase (HCT116-LUC-GFP) and CAF (CAF95, CAF62 and CAF95<sup>PDPN<sup>KD</sup></sup>) (four groups,  $n=24$ ). Mice in the fourth group started treatment (WP1066 20 mg/kg) 1 week after spleen injection (Fig. 6A). The body weight of mice and *in vivo* imaging were recorded during the treatment cycle (3 weeks) (Fig. 6B, C,E). The results showed that knockdown of PDPN and inhibition of STAT3 pathway significantly inhibited tumour growth compared with control group (Fig. 6D). Furthermore, there was no significant difference in mice body weight, suggesting that WP1066 had no serious toxic effects on the mice body (Fig. 6E). Hematoxylin-eosin-stained liver sections results showed that the formation of metastases in the liver was significantly reduced after PDPN knockdown and WP1066 treatment, indicating that knockdown of PDPN and inhibition of STAT3 pathway can suppress tumor metastasis in colorectal cancer (Fig. 6F-H).

Next, to study the effect of WP1066 on the PDPN/CCL2/STAT3 feedback loop *in vivo*, we measured the serum CCL2 levels by ELISA, and the results showed that the serum CCL2 levels in low PDPN expression group and WP1066 group were significantly decreased (Fig. 6I). In addition, after 2 weeks of treatment, we collected the spleens and detected the effect of WP1066 by IHC and IF (Fig. 6J, K). The IHC results showed that the expression of CD31 and ERG were significantly decreased after PDPN

knockdown and WP1066 treatment, while FAP expression had no significant difference (Fig. 6J, Fig. S5B, C). This means that WP1066 did not affect the number of CAF, but can inhibit the effect of angiogenesis *in vivo*. Notably, the change of PDPN expression indicated that WP1066 could down-regulate PDPN expression by inhibiting the activation of STAT3 signaling pathway, thus altering the pro-angiogenic heterogeneity of CAF and exerting inhibitory effect of angiogenesis. At the same time, Immunofluorescence further illustrated the inhibitory effect of WP1066 and PDPN knockdown in PDPN/CCL2/STAT3 feedback loop. The two treatments not only down-regulate PDPN expression in CAF, but also inhibit angiogenesis caused by STAT3 signaling pathway activation, implying that PDPN/CCL2/STAT3 feedback loop is a dominant mechanism by which WP1066 reverses PDPN<sup>high</sup> CAF-mediated pro-angiogenic heterogeneity (Fig. 6K).

These data suggest that PDPN is a specific marker of CAF with pro-angiogenic function, CAF with high PDPN expression can up-regulate CCL2 secretion and activate STAT3 pathway to promote angiogenesis. Besides, WP1066 was verified *in vivo* to inhibit angiogenesis by regulating CAF functional heterogeneity in PDPN/CCL2/STAT3 feedback loop, thus playing a role of inhibiting tumor growth and metastasis in liver metastasis model.

## Discussion

Accumulating studies have shown that CAF (cancer-associated fibroblast) heterogeneity predicts a poor prognosis in cancer patients [26]. Single-cell transcriptomic analysis have revealed the existence of various CAF subpopulations with distinct phenotypes and functions in pancreatic, breast and colorectal cancers. For example, myofibroblastic CAF (myCAF), inflammatory CAF (iCAF), antigen-presenting CAF (apCAF) and other different types of CAF play different functions and roles in these cancers [27–29]. A subpopulation of CAF tightly vessel-associated has also been observed and identified in breast cancer, which was termed vascular CAF (vCAF) [11]. Similarly, CAF has been suggested to be a major player in tumour angiogenesis, which can promote angiogenesis through the secretion of cytokines including VEGFA, PDGFC, SDF1, WNT2 and WNT5a [30–33]. However, in view of the fact that CAF markers and the mechanism of CAF-mediated tumor angiogenesis are still unclear, the establishment of CAF-targeted therapy still remains a series of challenges. In this study, we found significant differences in the pro-angiogenic function of CAF in colorectal cancer patients. To this end, we further explored the specific mechanisms by which CAF functional heterogeneity leads to angiogenesis.

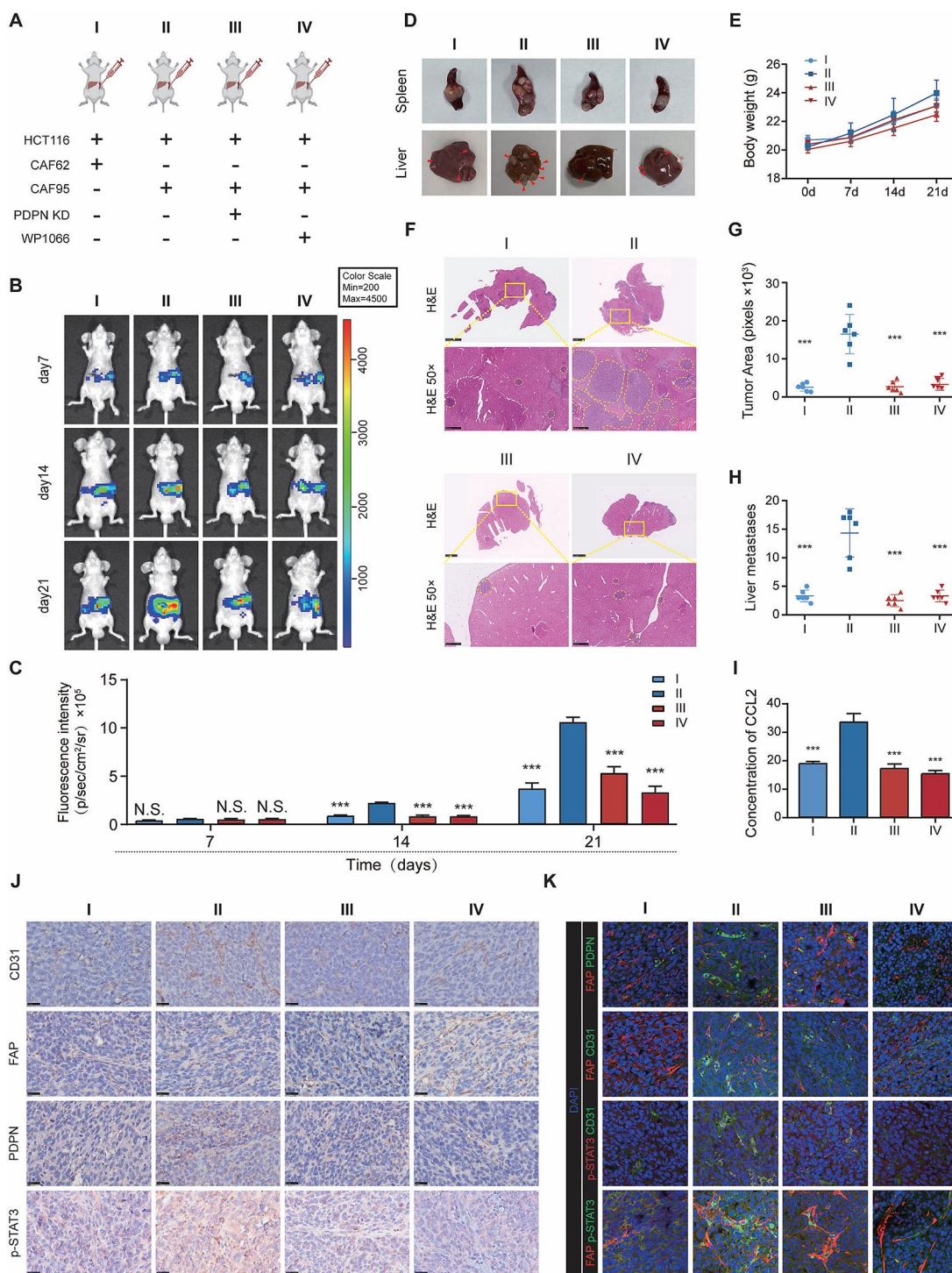
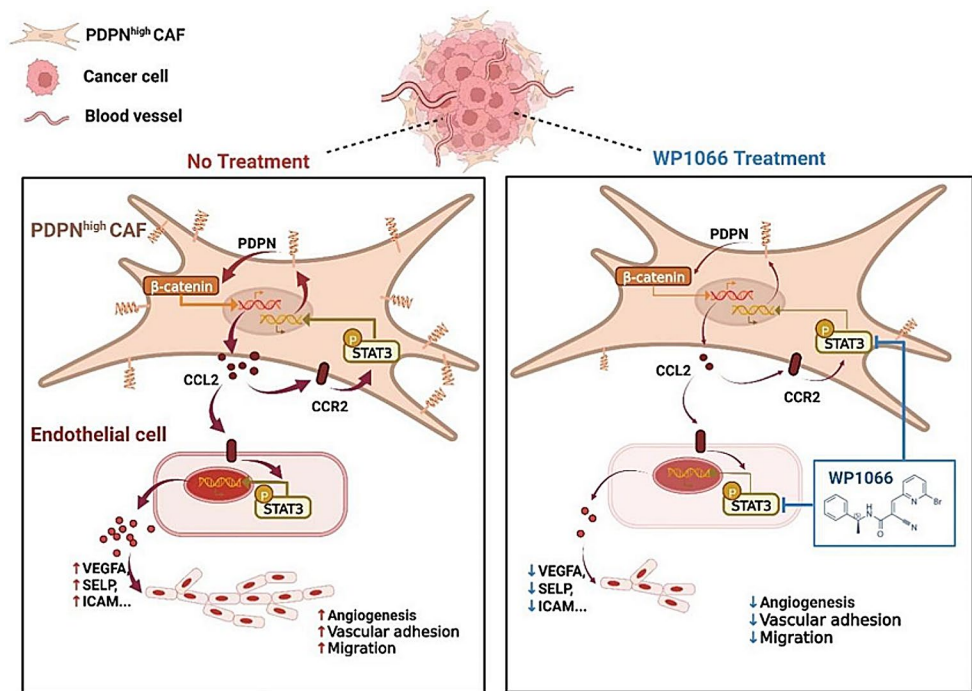


**Fig. 6** Inhibiting PDPN/CCL2/STAT3 feedback loop of CAF suppresses tumor metastasis by reducing angiogenesis in vivo. **(A)** Scheme and group of treatments with PDPN knockdown and WP1066. **(B, C)** Tumor growth and metastasis was visualized by an in vivo imaging system from day 7 to day 21. **(D)** Representative images of tumors in spleen and liver. **(E)** body weights of mice from day 0 to day 21. **(F)**

Representative images of H&E-stained liver tissue in four groups. **(G, H)** Tumor area and metastasis number in the liver. **(I)** ELISA detection of CCL2 expression level in mice serum. **(J-K)** Representative images of the IHC and IF analysis of FAP, PDPN, p-STAT3 and CD31 in mouse spleen tissues. Scale bar: 25 μm The results are presented as the mean (SD)

**Fig. 7** Schematic diagram of the mechanism of STAT3 inhibitor WP1066 regulating CAF-mediated angiogenesis in colorectal cancer



As a commonly CAF marker, PDPN is highly expressed in a variety of cancers, including breast cancer [15], lung cancer [12], pancreatic cancer [16] and so on. Clinicopathological results show that high PDPN expression is significantly related to the poor prognosis of cancer. Notably, studies have shown that high PDPN expression is positively correlated with angiogenesis, which may affect tumor vascularization [17]. In our study, we extracted primary CAFs from different colorectal cancer patients tissue and divided four primary CAFs into two subpopulations with differential PDPN expression by transcriptome sequencing analysis. We found that the CAF subpopulation with high PDPN expression (PDPN<sup>high</sup> CAF) was significantly associated with angiogenesis. Knockdown of PDPN significantly down-regulated the CAF-mediated pro-angiogenic effect. Therefore, our studies confirm that PDPN can serve as a specific marker to distinguish CAFs-mediated pro-angiogenic functional heterogeneity.

Previous studies have reported that PDPN can up-regulate the Wnt/β-catenin signaling, causing nuclear translocation of β-catenin to drive angiogenesis [18]. In our study, whole transcriptome sequencing showing the enrichment of Wnt signaling pathways and up-regulation of Wnt-related pathway proteins in PDPN<sup>high</sup> CAF. Meanwhile, It has been suggested that PDPN<sup>high</sup> CAF can release angiogenic factors and promote vascularization [34]. Wnt/β-catenin signaling can activate relevant chemokines [19]. Our results suggest that PDPN<sup>high</sup> CAF may secrete cytokine through nuclear translocation of β-catenin, and we further demonstrate that CCL2 plays a key role as a cytokine in the pro-angiogenic

function of PDPN<sup>high</sup> CAF. Thus, these data demonstrate that PDPN<sup>high</sup> CAF up-regulates CCL2 secretion to promote angiogenesis through the Wnt/β-catenin signaling pathway in colorectal cancer.

Chemokines have been reported to induce STAT3 activation [35, 36], such as CCL2, which is associated with the progression of various cancers and can also promote tumor growth through a variety of mechanisms [37]. STAT3 is a pleiotropic transcription factor, activation of the STAT3 signaling pathway in CAF can promote angiogenesis [20, 25]. In our study, we found that PDPN<sup>high</sup> CAF can regulate STAT3 phosphorylation in HUVEC through paracrine CCL2 to mediate angiogenesis. Moreover, we also found that PDPN<sup>high</sup> CAF can regulate its heterogeneity through autocrine CCL2 to form a PDPN/CCL2/STAT3 feedback loop and maintain the pro-angiogenic functional subtype of CAF.

Single cell sequencing and immunohistochemical staining of clinical specimens confirmed that PDPN could specifically mark the CAF subtype with high pro-angiogenic function and the PDPN/CCL2/STAT3 feedback loop in PDPN<sup>high</sup> CAF affects the functional heterogeneity of CAF. Antiangiogenic therapy is an important strategy for the treatment of CRC. WP1066 has been proved to inhibit tumor angiogenesis in preclinical models and is an effective STAT3 inhibitor in vivo and in vitro. In our study, based on the dual activation of STAT3 in CAF and HUVEC, we found that WP1066 can directly inhibit angiogenesis in HUVEC by inhibiting STAT3 phosphorylation, and can also alter CAF pro-angiogenic functional heterogeneity to

inhibit angiogenesis by down-regulating PDPN expression. Similarly, we established a liver metastasis model *in vivo*, and we found that WP1066 can effectively inhibit angiogenesis and tumor metastasis of CRC through mediating the PDPN/CCL2/STAT3 feedback loop.

In conclusion, our results reveal CAF functional heterogeneity in terms of promoting angiogenesis in colorectal cancer. PDPN can specifically mark CAF subpopulations with strong pro-angiogenic function. PDPN<sup>high</sup> CAF maintains its heterogeneity by activating the PDPN/CCL2/STAT3 feedback loop through autocrine CCL2, and activates the STAT3 pathway to promote angiogenesis by paracrine CCL2 in HUVEC. Based on the above mechanisms, WP1066 can regulate CAF heterogeneity and inhibit angiogenesis by inhibiting PDPN/CCL2/STAT3 feedback loop. Thus, our therapeutic approach based on STAT3 target provides a potential therapeutic target for inhibiting tumour metastasis and growth of colorectal cancer.

**Supplementary Information** The online version contains supplementary material available at <https://doi.org/10.1007/s10456-024-09941-9>.

**Acknowledgements** This study was mainly supported by Wenzhou Science and Technology Project (No.Y20220178 & No.Y20220016).

**Author contributions** D Y, H X and J Z have contributed equally to the writing process of this manuscript. K X designed and guided the review. D Y, H X, J Z and K X wrote and edited the manuscript. K F, Z Z helped with reference collection and draw the figures. All authors read and approved the final manuscript.

**Data availability** No datasets were generated or analysed during the current study.

## Declarations

**Ethics approval and consent to participate** All animal experiments in this study were evaluated and approved by the Animal Ethics Committee of Putuo District Center Hospital, Shanghai (Putuo Hospital, Shanghai University of Traditional Chinese Medicine).

**Competing interests** The authors declare no competing interests.

## References

- Zhu X, Wang F, Wu X, Li Z, Wang Z, Ren X, Zhou Y, Song F, Liang Y, Zeng Z, Liao W, Ding Y, Liao W, Liang L (2020) FBX8 promotes metastatic dormancy of colorectal cancer in liver. *Cell Death Dis* 11(8):622
- Arnold M, Sierra MS, Laversanne M et al (2017) Global patterns and trends in colorectal cancer incidence and mortality. *Gut* 66(4):683–691
- Arnold M, Abnet CC, Neale RE et al (2020) Global burden of 5 major types of gastrointestinal Cancer. *Gastroenterology* 159(1):335–349
- Czekay RP, Cheon DJ, Samarakoon R, Kutz SM, Higgins PJ (2022) Cancer-Associated fibroblasts: mechanisms of Tumor Progression and Novel therapeutic targets. *Cancers* 14(5):1231
- Gascard P, Tlsty TD (2016) Carcinoma-associated fibroblasts: orchestrating the composition of malignancy. *Genes Dev* 30(9):1002–1019
- Xing F, Saidou J, Watabe K (2010) Cancer associated fibroblasts (CAFs) in tumor microenvironment. *Front Biosci (Landmark Ed)* 15(1):166–179
- Chen X, Song E (2019) Turning foes to friends: targeting cancer-associated fibroblasts. *Nat Rev Drug Discov* 18(2):99–115
- Kobayashi H, Enomoto A, Woods SL et al (2019) Cancer-associated fibroblasts in gastrointestinal cancer. *Nat Rev Gastroenterol Hepatol* 16(5):282–295
- Liu T et al (2019) Cancer-associated fibroblasts: an emerging target of anti-cancer immunotherapy. *J Hematol Oncol* 121:86
- Bu L et al (2019) Biological heterogeneity and versatility of cancer-associated fibroblasts in the tumor microenvironment. *Oncogene* 3825:4887–4901
- Bartoschek M, Oskolkov N, Bocci M et al (2018) Spatially and functionally distinct subclasses of breast cancer-associated fibroblasts revealed by single cell RNA sequencing. *Nat Commun* 9(1):5150
- Hoshino A, Ishii G, Ito T et al (2011) Podoplanin-positive fibroblasts enhance lung adenocarcinoma tumor formation: podoplanin in fibroblast functions for tumor progression. *Cancer Res* 71(14):4769–4779
- Sasaki K, Sugai T, Ishida K et al (2018) Analysis of cancer-associated fibroblasts and the epithelial-mesenchymal transition in cutaneous basal cell carcinoma, squamous cell carcinoma, and malignant melanoma. *Hum Pathol* 79(1):1–8
- Suzuki J, Aokage K, Neri S et al (2021) Relationship between podoplanin-expressing cancer-associated fibroblasts and the immune microenvironment of early lung squamous cell carcinoma. *Lung Cancer* 153(1):1–10
- Pula B, Jethon A, Piotrowska A, Gomulkiewicz A et al (2011) Podoplanin expression by cancer-associated fibroblasts predicts poor outcome in invasive ductal breast carcinoma. *Histopathology* 59(6):1249–1260
- Shindo K, Aishima S, Ohuchida K et al (2013) Podoplanin expression in cancer-associated fibroblasts enhances tumor progression of invasive ductal carcinoma of the pancreas. *Mol Cancer* 12(1):168
- Li J, Chen H, Li X et al (2017) Co-expression of podoplanin and fibroblast growth factor 1 predicts poor prognosis in patients with lung squamous cell carcinoma. *Mol Med Rep* 16(2):1643–1652
- Bresson L, Faraldo MM, Di-Cicco A et al (2018) Podoplanin regulates mammary stem cell function and tumorigenesis by potentiating Wnt/ $\beta$ -catenin signaling. *Development* 145(4):160382
- Kasprzak A (2020) Angiogenesis-related functions of wnt signaling in colorectal carcinogenesis. *Cancers (Basel)* 12(12):3601
- Heichler C, Scheibe K, Schmied A et al (2020) STAT3 activation through IL-6/IL-11 in cancer-associated fibroblasts promotes colorectal tumour development and correlates with poor prognosis. *Gut* 69(7):1269–1282
- Shen W, Zhang X, Tang J et al (2021) CCL16 maintains stem cell-like properties in breast cancer by activating CCR2/GSK3 $\beta$ / $\beta$ -catenin/OCT4 axis. *Theranostics* 11(5):2297–2317
- Tian DS, Peng J, Murugan M et al (2017) Chemokine CCL2-CCR2 signaling induces neuronal cell death via STAT3 activation and IL-1 $\beta$  production after Status Epilepticus. *J Neurosci* 37(33):7878–7892
- Priester M, Copanaki E, Vafaizadeh V et al (2013) STAT3 silencing inhibits glioma single cell infiltration and tumor growth. *Neuro Oncol* 15(7):840–852



24. Fujii M, Honma M, Takahashi H et al (2013) Intercellular contact augments epidermal growth factor receptor (EGFR) and signal transducer and activator of transcription 3 (STAT3)-activation which increases podoplanin-expression in order to promote squamous cell carcinoma motility. *Cell Signal* 25(4):760–765
25. Allam A, Yakou M, Pang L, Ernst M, Huynh J (2021) Exploiting the STAT3 Nexus in Cancer-Associated fibroblasts to Improve Cancer Therapy. *Front Immunol* 12(1):767939
26. Czekay RP, Cheon DJ, Samarakoon R, Kutz SM, Higgins PJ (2022) Cancer-Associated fibroblasts: mechanisms of Tumor Progression and Novel therapeutic targets. *Cancers (Basel)* 14(5):1231
27. Elyada E, Bolisetty M, Laise P et al (2019) Cross-species single-cell analysis of pancreatic ductal adenocarcinoma reveals antigen-presenting cancer-associated fibroblasts. *Cancer Discov* 9:1102–1123
28. Sebastian A, Hum NR, Martin KA et al (2020) Single-cell transcriptomic analysis of tumor-derived fibroblasts and normal tissue-resident fibroblasts reveals fibroblast heterogeneity in breast cancer. *Cancers (Basel)* 12:1307
29. Li H, Courtois ET, Sengupta D et al (2017) Reference component analysis of single-cell transcriptomes elucidates cellular heterogeneity in human colorectal tumors. *Nat Genet* 49:708–718
30. De Palma M, Biziato D, Petrova TV (2017) Microenvironmental regulation of tumour angiogenesis. *Nat Rev Cancer* 17:457–474
31. Crawford Y, Kasman I, Yu L, Zhong C, Wu X, Modrusan Z et al (2009) PDGF-C mediates the angiogenic and tumorigenic properties of fibroblasts associated with tumors refractory to anti-VEGF treatment. *Cancer Cell* 15:21–34
32. Orimo A, Gupta PB, Sgroi DC, Arenzana-Seisdedos F, Delaunay T, Naeem R et al (2005) Stromal fibroblasts present in invasive human breast carcinomas promote tumor growth and angiogenesis through elevated SDF-1/CXCL12 secretion. *Cell* 121:335–348
33. Unterleuthner D, Neuhold P, Schwarz K, Janker L, Neuditschko B, Nivarthi H et al (2020) Cancer-associated fibroblast-derived WNT2 increases tumor angiogenesis in colon cancer. *Angiogenesis* 23:159–177
34. Hu G, Zhong K, Chen W, Wang S, Huang L (2018) Podoplanin-positive cancer-associated fibroblasts predict poor prognosis in lung cancer patients. *Onco Targets Ther* 11(1):5607–5619
35. Van Coillie E, Van Damme J, Opdenakker G (1999) The MCP eotaxin subfamily of CC chemokines. *Cytokine Growth Factor Rev* 10(1):61–86
36. Bianconi V, Sahebkar A, Atkin SL, Pirro M (2018) The regulation and importance of monocyte chemoattractant protein-1. *Curr Opin Hematol* 25(1):44–51
37. Korbecki J, Kojder K, Simińska D et al (2020) CC chemokines in a Tumor: a review of Pro-cancer and Anti-cancer properties of the ligands of receptors CCR1, CCR2, CCR3, and CCR4. *Int J Mol Sci* 21(21):8412

**Publisher's Note** Springer Nature remains neutral with regard to jurisdictional claims in published maps and institutional affiliations.

Springer Nature or its licensor (e.g. a society or other partner) holds exclusive rights to this article under a publishing agreement with the author(s) or other rightsholder(s); author self-archiving of the accepted manuscript version of this article is solely governed by the terms of such publishing agreement and applicable law.